ACS Catalysis

Letter

pubs.acs.org/acscatalysis

Genetic Optimization of the Catalytic Efficiency of Artificial Imine Reductases Based on Biotin−Streptavidin Technology

Fabian Schwizer, Valentin Köhler, Marc Dürrenberger, Livia Knörr, and Thomas R. Ward*

Department of Chemistry, University of Basel, Spitalstrasse 51, CH-4056 Basel, Switzerland

Supporting Information

ABSTRACT: Artificial metalloenzymes enable the engineering of the reaction microenvironment of the active metal catalyst by modification of the surrounding host protein. We report herein the optimization of an artificial imine reductase (ATHase) based on biotin−streptavidin technology. By introduction of lipophilic amino acid residues around the active site, an 8-fold increase in catalytic efficiency compared with the wild type imine reductase was achieved. Whereas substrate inhibition was encountered for the free cofactor and wild type ATHase, two engineered systems exhibited classical Michaelis−Menten kinetics, even at substrate concentrations of 150 mM with measured rates up to 20 min^{-1}.

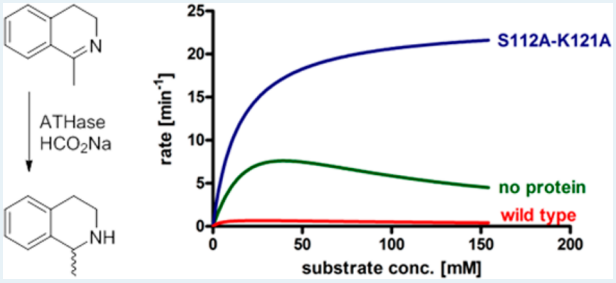

KEYWORDS: *artificial metalloenzymes, imine reduction, transfer hydrogenation, biotin−streptavidin technology, genetic optimization, saturation kinetics*

INTRODUCTION

Artificial metalloenzymes result from incorporation of an organometallic catalyst precursor within a host protein.[1−10] In analogy to natural metalloenzymes, both the metal coordination and the substrate-binding sphere around the catalytic site can be defined and are amenable to optimization. In the past 10 years, we and others have relied on the biotin−(strept)avidin technology for the creation of artificial metalloenzymes.

Artificial metalloenzymes offer new opportunities to improve catalytic efficiency and selectivity. For this purpose, both chemical modification of the first coordination sphere and mutation of the host protein (i.e., the reaction environment) can be used to optimize the performance of the artificial metalloenzyme.[11] Although highly enantioselective artificial metalloenzymes have been reported for a variety of transformations, they often display lower activity than the "protein-free" metal cofactor.

To overcome this challenge, approaches relying on fine-tuning of the first or second coordination sphere around the metal may be envisaged. We recently described first coordination sphere engineering approaches whereby a biotinylated catalyst precursor was activated upon incorporation within streptavidin. This was achieved thanks to the introduction of a coordinating amino acid capable of binding and activating the artificial cofactor.[12,13]

Herein, we present our efforts to improve catalytic efficiency by genetically fine-tuning the reaction environment in direct proximity of the metal catalyst in an artificial imine reductase based on biotin−streptavidin technology, Scheme 1.

RESULTS AND DISCUSSION

With the aim of quantifying the effect of streptavidin isoforms (hereafter, Sav) on the catalytic performance of the biotinylated d^6 piano stool complex [Cp*Ir(biot-*p*-L)Cl], we set out to determine the saturation kinetic behavior for the asymmetric transfer hydrogenation of 1-methyl-3,4-dihydroisoquinoline **1** to the corresponding enantioenriched amine **2** (Scheme 1), striving for a higher catalytic efficiency[14] rather than an improved enantioselectivity.[15,16]

As a starting point, we determined the kinetic profiles for the isolated catalyst precursor [Cp*Ir(biot-*p*-L)Cl] as well as for the artificial metalloenzyme resulting from its incorporation within WT Sav, Figure 2 and Table 1 (see the Supporting Information, SI, for details). As can be appreciated from these data, compared with the free [Cp*Ir(biot-*p*-L)Cl] cofactor, the artificial metalloenzyme based on WT Sav displays a 20-fold decrease in rate, as reflected by k_{obs} and k_{cat}, respectively (21 ± 7 vs 1 ± 0.1 min^{-1}), accompanied by a decrease in K_M (34 ± 16 vs 5.0 ± 1.6 mM). In addition, both systems suffer from substrate inhibition (K_i = 45 ± 20 vs 131 ± 27 mM).[17] Similar inhibition effects have been reported for the transfer hydrogenation of carbonyl compounds.[18−20] Because the initial rates are determined at low conversion, we speculate that the binding of a second substrate molecule in the active site of the ATHase is responsible for the observed rate decrease, rather than product or CO_2 inhibition.[21] A possible explanation for the inhibition of the free metal cofactor might be found in the

Received: June 5, 2013
Revised: July 4, 2013
Published: July 8, 2013

   dx.doi.org/10.1021/cs400428r | ACS Catal. 2013, 3, 1752−1755

Scheme 1. Reduction of a Cyclic Imine[a] with ATHases Based on Streptavidin Isoforms[b]

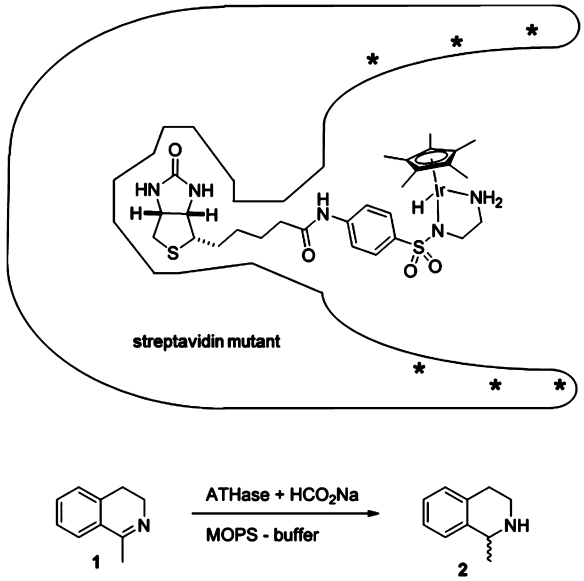

[a]Asymmetric transfer hydrogenation of 1-methyl-3,4-dihydroisoquinoline **1** with the engineered metalloenzymes. MOPS = 3-morpholinopropanesulfonic acid. [b]Artificial imine reductase (ATHase), resulting from incorporation of a biotinylated cofactor [Cp*Ir(biot-*p*-L)Cl] within streptavidin. Genetic optimization (*) allows improvement of the catalytic performance of the artificial metalloenzyme.

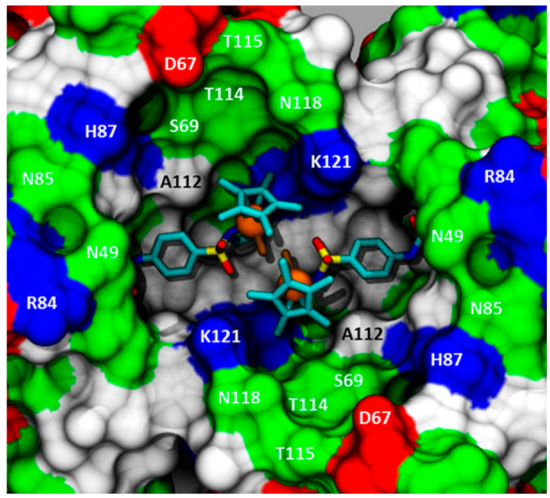

Figure 1. X-ray structure (PDB ID 3PK2) of homotetrameric streptavidin mutant S112A with the bound cofactor [Cp*Ir(biot-*p*-L)Cl]. The close-up view of the surface representation highlights the symmetry-related artificial cofactor (stick representation; Ir, orange sphere) and close-lying amino acid residues (color code: red = acidic, blue = basic, green = polar, white = apolar).

reversible coordination of the imine substrate to the 16-electron intermediate.[22,23]

To enable efficient catalysis at *very low* substrate concentrations, as encountered in a prospective physiological context (<1 mM), we hypothesized that increasing the hydrophobicity in the biotin-binding vestibule, where the {Cp*Ir} moiety is located, may increase the local concentration of substrate **1**.[24]

Inspection of the X-ray structure of [Cp*Ir(biot-*p*-L)-Cl]·S112A Sav (Figure 1) reveals three cationic (R84, H87, and K121), one anionic (D67), and six polar (N49, S69, N85, T114, T115, N118) residues located in the proximity of the piano stool moiety.[16] In previous studies, we identified position S112 as particularly propitious for the optimization of enantioselectivity: [Cp*Ir(biot-*p*-L)Cl]·S112A Sav yields up to 96% ee for the reduction of cyclic imines.[16] In addition, mutations attempted at H87 suggest that this residue is critical to the proper folding of Sav.[25,26] On the basis of these considerations and with the aim of deconvoluting individual contributions, lipophilic mutations were introduced sequentially. Starting from WT Sav, two series were designed: (i) WT Sav → S112A → S112A-K121A → R84A-S112A-K121A and (ii) WT → S112A → S112A-K121L → D67V-S112A-K121L. The mutations were introduced using the QuikChange site-directed mutagenesis protocol (Stratagene, modified by Zheng et al.[27]). The Sav isoforms were recombinantly expressed in *Escherichia coli* and purified using affinity chromatography on a 2-iminobiotin sepharose column.[28]

The saturation kinetic behavior for all artificial imine reductases was determined in triplicate. To quench the reaction prior to analysis, L-glutathione (final concentration: 83 mM) was added to the reaction mixture. Analysis was performed by reversed phase HPLC using 2-(3,4-dimethoxyphenyl)ethanol as internal standard. An excess of free biotin-binding sites vs Ir cofactor was employed in all cases; the possible effect caused by a variation in ratio was not investigated. The kinetic results are presented in Figure 2 and are collected in Table 1.

Substitution of the cationic residue at position K121 for a hydrophobic residue (e.g., alanine, K121A) has a dramatic effect on the catalytic efficiency: it significantly improves the k_{cat} (20 ± 3 vs 1 ± 0.1 min^{-1} for WT ATHase), nearly restoring that of the isolated cofactor. The K_M, however, increases compared with WT ATHase (12 ± 3 vs 5.0 ± 1.6 mM). Although substrate **1** may appear hydrophobic at first sight, we and others assume that it is partly protonated under catalytic

Table 1. Kinetic Parameters of the Reduction of Imine 1, Using ATHases Based on Streptavidin Isoforms

entry	mutation	k_{cat} (min^{-1})	K_M (mM)	K_i[a] (mM)	k_{cat}/K_M (min^{-1} mM^{-1})	*ee*[b] (%) (*R*) enantiomer
1	no protein	20.9 ± 6.5[c]	34.4 ± 15.6	45.1 ± 19.9	0.61	*rac.*
2	wild type	0.95 ± 0.09	5.04 ± 1.59	131 ± 27	0.19	60
3	S112A-K121A	23.7 ± 0.8	14.9 ± 2.1		1.59	47
4	S112A-K121L	17.8 ± 0.4	12.4 ± 1.1		1.44	45
5	R84A-S112A-K121A	37.6 ± 4.6	29.3 ± 6.0	187 ± 53	1.28	51
6	D67 V−S112A-K121L	12.2 ± 2.3	12.9 ± 5.8	411 ± 324	0.94	30
7	K121A	19.7 ± 3.0[d]	11.5 ± 2.6[d]	19.6 ± 4.4[d]	1.71	48

[a]Determined by applying the Haldane equation for substrate inhibition.[17] [b]Determined by chiral phase HPLC at 4.8 mM initial substrate concentration and >85% conversion (see the Supporting Information, for details). [c]Termed k_{obs} instead of k_{cat}. [d]Values taken from Köhler et al.[15]

dx.doi.org/10.1021/cs400428r | *ACS Catal.* 2013, 3, 1752−1755

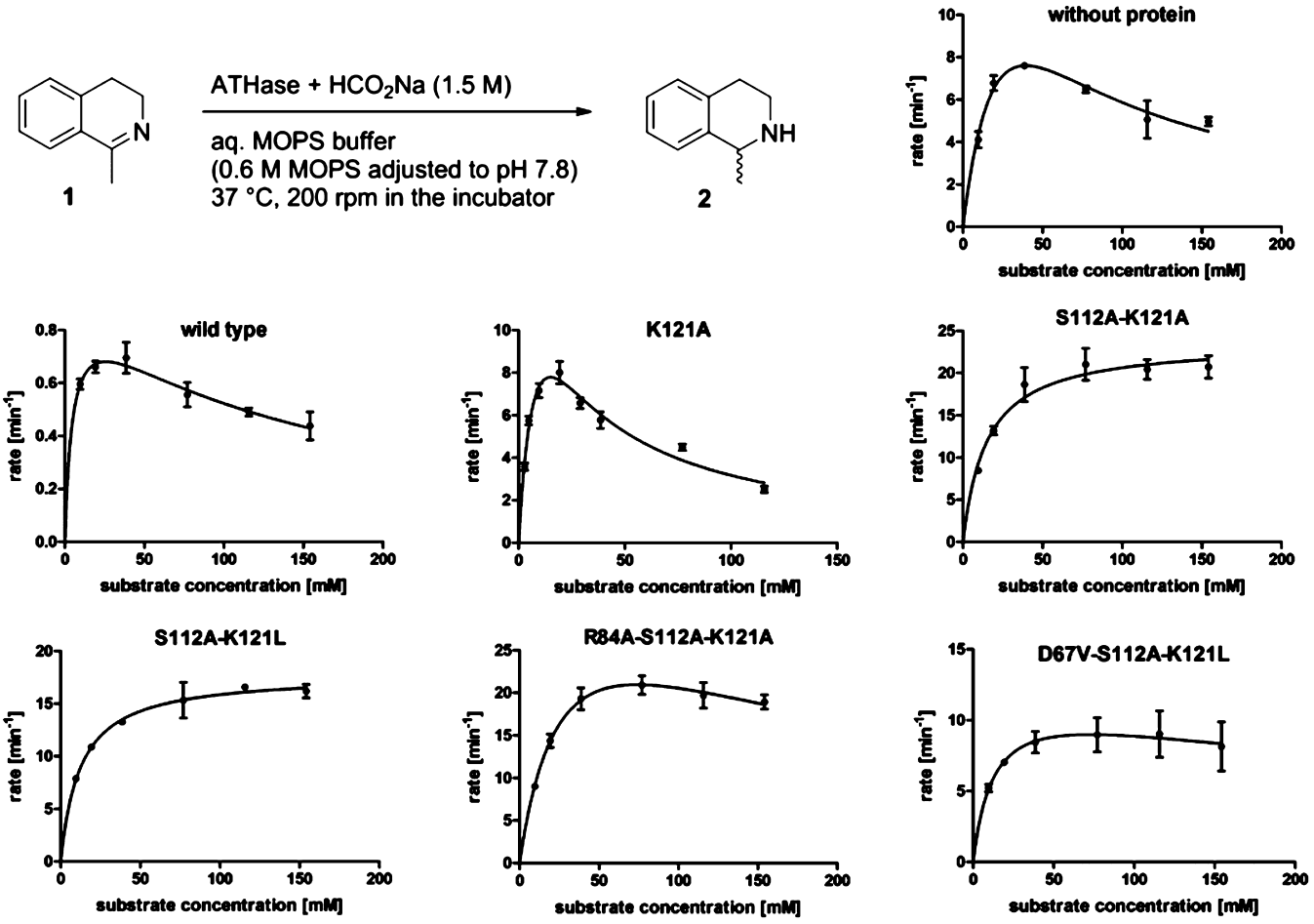

Figure 2. Saturation kinetic profiles of ATHases based on incorporation of [Cp*Ir(biot-*p*-L)Cl] in various streptavidin isoforms for the reduction of imine **1** (reaction scheme is illustrated in the top left corner of the figure). Error bars show ±1 standard deviation. The kinetic parameters (k_{cat}, K_M, and K_i) are collected in Table 1.

conditions at pH 7.8, and in fact, it is the iminium ion that is involved in the transition state.[29−35]

Having identified a favorable substitution at position K121,[15] an additional mutation at position S112 was introduced. The ATHase derived from both double mutants S112A-K121A and S112A-K121L (Table 1, entries 3 and 4) display similar k_{cat} values (23.7 ± 0.8 and 17.8 ± 0.4 min^{-1}, respectively) and K_M values (15 ± 2 and 12 ± 1 mM, respectively). We thus conclude that it is the nature (cationic vs hydrophobic) but not the size of the amino acid residue at position K121 (alanine or leucine) that plays a determining role in the catalytic performance. The catalytic efficiency (k_{cat}/K_M) of both double mutants is significantly higher than that of either the free cofactor or of the WT ATHase. Although slightly lower than the theoretical catalytic efficiency of [Cp*Ir(biot-*p*-L)-Cl]·K121A Sav, no substrate inhibition is observed for the double mutants, which accordingly show higher effective rates.

Next, triple mutants were prepared. Substitution of the cationic arginine for a hydrophobic alanine at position R84 affords the corresponding ATHase [Cp*Ir(biot-*p*-L)Cl]·R84A-S112A-K121A (Table 1, entry 5). In this case, a k_{cat} = 38 ± 5 min^{-1} and K_M = 29 ± 6 mM is computed. The k_{cat} is thus significantly improved compared to the free cofactor, accompanied by a reduction in substrate inhibition (K_i = 187 ± 53 vs 45 ± 20 mM for the free cofactor). Substitution of an aspartate residue by a valine at position D67 is less effective at improving catalytic efficiency (Table 1, entry 6).

Considering the ratio k_{cat}/K_M as a widely used, albeit imperfect, measure of catalytic efficiency of an enzyme,[14] it was shown that all lipophilic mutants are more efficient than the WT Sav-based ATHase (between 5 and 9 times higher efficiency). The best efficiency in the absence of substrate inhibition is obtained for the double mutant S112A-K121A (Table 1, entry 3) with a ratio of 1.59 min^{-1} mM^{-1}, compared with 0.19 min^{-1} mM^{-1} for WT Sav.

The hypothesis that the reduction of imine **1** takes place via an iminium ion lends support to the increase in catalytic efficiency when the cationic lysine residue at position K121 is substituted by an apolar residue.[29−32] Furthermore, it allows rationalization of the observation that the triple mutant D67V-S112A-K121L displays a lower k_{cat} than the corresponding double mutant S112A-K121L. Indeed, the aspartate residue may stabilize the cationic transition state. In contrast, substitution of the arginine at position R84 decreases electrostatic repulsion with the iminium ion, leading to a higher rate (Table 1, entry 5). It should be noted that mutant S112K, investigated previously, displays also a higher k_{cat} than WT Sav ATHase (5.4 ± 0.21 min^{-1} for S112K vs 1 ± 0.1 min^{-1} for WT).[15] The reaction, however, leads preferentially to the formation of the *S* enantiomer, whereas all ATHases investigated in this study yield preferentially the *R* enantiomer.

dx.doi.org/10.1021/cs400428r | *ACS Catal.* 2013, 3, 1752−1755

This suggests a different arrangement of the complex in the active site as supported by inspection of mutant ATHase X-ray structures.[16,36]

In this exploratory study, we have achieved a nearly 40-fold increase in k_{cat}, but only a 6-fold increase in K_M for the triple mutant R84A-S112A-K121A when compared to [Cp*Ir(biot-*p*-L)Cl]·WT Sav. As a result, the catalytic efficiencies (k_{cat}/K_M) of the lipophilic ATHases are, despite the modest increase in K_M, significantly improved compared with either the free cofactor or the wild-type ATHase [Cp*Ir(biot-*p*-L)Cl]·WT Sav. Importantly, the introduction of an additional mutation S112A in the double mutants S112A-K121A and S112A-K121L allowed overcoming of the substrate inhibition, encountered, for example, with the free cofactor or the K121A single-mutant-based ATHase. As a result, substantially increased effective rates are achieved, a feature reminiscent of natural enzymes.

OUTLOOK

Genetic optimization of the second coordination sphere around the {Cp*Ir} moiety allows improvement of the catalytic performance of an artificial imine reductase based on the biotin−streptavidin technology. Increasing the lipophilic character of the active site leads to a significant increase in the k_{cat}, accompanied by a less pronounced increase in the K_M of the resulting artificial metalloenzymes. This optimization was achieved by screening only a handful of mutants and limited structural knowledge. We anticipate that computing the structure and energetics of both the [enzyme·substrate] and the corresponding transition state of the reaction will allow further rational improvement of the catalytic performance of such artificial metalloenzymes.

ASSOCIATED CONTENT

Supporting Information

Design and expression of streptavidin mutants, experimental procedure of the kinetic measurements. This information is available free of charge via the Internet at http://pubs.acs.org/.

AUTHOR INFORMATION

Corresponding Author

*E-mail: thomas.ward@unibas.ch.

Notes

The authors declare no competing financial interest.

ACKNOWLEDGMENTS

This research was funded by the Swiss National Science Foundation (SNF Grant 200020_144354) and the Swiss Nanoscience Institute, Basel. We thank Dr. Marc Creus for help in designing the primers, Charles Cantor for the streptavidin gene, and Umicore for a loan of $[Cp^*IrCl_2]_2$.

REFERENCES

(1) Wilson, M. E.; Whitesides, G. M. *J. Am. Chem. Soc.* **1978**, *100*, 306−307.
(2) Deuss, P. J.; den Heeten, R.; Laan, W.; Kamer, P. C. J. *Chem.—Eur. J.* **2011**, *17*, 4680−4698.
(3) Ward, T. R. *Acc. Chem. Res.* **2011**, *44*, 47−57.
(4) Bos, J.; Fusetti, F.; Driessen, A. J. M.; Roelfes, G. *Angew. Chem., Int. Ed.* **2012**, *51*, 7472−7475.
(5) Qi, D.; Tann, C.-M.; Haring, D.; Distefano, M. D. *Chem. Rev.* **2001**, *101*, 3081−3111.
(6) Köhler, V.; Wilson, Y. M.; Lo, C.; Sardo, A.; Ward, T. R. *Curr. Opin. Biotechnol.* **2010**, *21*, 744−752.
(7) Ueno, T.; Abe, S.; Yokoi, N.; Watanabe, Y. *Coord. Chem. Rev.* **2007**, *251*, 2717−2731.
(8) Reetz, M. T.; Rentzsch, M.; Pletsch, A.; Maywald, M.; Maiwald, P.; Peyralans, J. J. P.; Maichele, A.; Fu, Y.; Jiao, N.; Hollmann, F.; Mondière, R.; Taglieber, A. *Tetrahedron* **2007**, *63*, 6404−6414.
(9) Loosli, A.; Rusbandi, U. E.; Gradinaru, J.; Bernauer, K.; Schlaepfer, C. W.; Meyer, M.; Mazurek, S.; Novic, M.; Ward, T. R. *Inorg. Chem.* **2006**, *45*, 660−668.
(10) Wang, C.; Li, C.; Wu, X.; Pettman, A.; Xiao, J. *Angew. Chem., Int. Ed.* **2009**, *48*, 6524−6528.
(11) Rosati, F.; Roelfes, G. *ChemCatChem* **2010**, *2*, 916−927.
(12) Hyster, T. K.; Knörr, L.; Ward, T. R.; Rovis, T. *Science (Washington, DC, U.S.)* **2012**, *338*, 500−503.
(13) Zimbron, J. M.; Heinisch, T.; Schmid, M.; Hamels, D.; Nogueira, E. S.; Schirmer, T.; Ward, T. R. *J. Am. Chem. Soc.* **2013**, *135*, 5384−5388.
(14) A note of caution is appropriate when k_{cat}/K_M values are used to compare catalytic efficiencies: Eisenthal, R.; Danson, M. J.; Hough, D. W. *Trends Biotechnol.* **2007**, *25*, 247−249.
(15) Köhler, V.; Wilson, Y. M.; Dürrenberger, M.; Ghislieri, D.; Churakova, E.; Quinto, T.; Knörr, L.; Häussinger, D.; Hollmann, F.; Turner, N. J.; Ward, T. R. *Nat. Chem.* **2013**, *5*, 93−99.
(16) Dürrenberger, M.; Heinisch, T.; Wilson, Y. M.; Rossel, T.; Nogueira, E.; Knörr, L.; Mutschler, A.; Kersten, K.; Zimbron, M. J.; Pierron, J.; Schirmer, T.; Ward, T. R. *Angew. Chem., Int. Ed.* **2011**, *50*, 3026−3029.
(17) Haldane, J. B. S. *Enzymes*, Longmans, Green and Co.: New York, 1930; reprinted by MIT Press, 1965; p 84.
(18) Heller, D.; de Vries, A. H. M.; de Vries, J. G. *Handbook of Homogeneous Hydrogenation*; de Vries, J. G., Elsevier, C. J., Eds.; Wiley-VCH: Weinheim, 2007; p 1483−1516.
(19) Wu, X.; Li, X.; Zanotti-Gerosa, A.; Pettman, A.; Liu, J.; Mills, A. J.; Xiao, J. *Chem.—Eur. J.* **2008**, *14*, 2209−2222.
(20) Wu, X.; Liu, J.; Di Tommaso, D.; Iggo, J. A.; Catlow, C. R. A.; Bacsa, J.; Xiao, J. *Chem.—Eur. J.* **2008**, *14*, 7699−7715.
(21) Strotman, N. A.; Baxter, C. A.; Brands, K. M. J.; Cleator, E.; Krska, S. W.; Reamer, R. A.; Wallace, D. J.; Wright, T. J. *J. Am. Chem. Soc.* **2011**, *133*, 8362−8371.
(22) Haack, K.-J.; Hashiguchi, S.; Fujii, A.; Ikariya, T.; Noyori, R. *Angew. Chem., Int. Ed.* **1997**, *36*, 285−288.
(23) Murata, K.; Konishi, H.; Ito, M.; Ikariya, T. *Organometallics* **2002**, *21*, 253−255.
(24) Matsuo, T.; Fukumoto, K.; Watanabe, T.; Hayashi, T. *Chem.—Asian J.* **2011**, *6*, 2491−2499.
(25) Reetz, M. T.; Peyralans, J. J. P.; Maichele, A.; Fu, Y.; Maywald, M. *Chem. Commun. (Cambridge, U. K.)* **2006**, 4318−4320.
(26) Köhler, V.; Mao, J.; Heinisch, T.; Pordea, A.; Sardo, A.; Wilson, Y. M.; Knörr, L.; Creus, M.; Prost, J.-C.; Schirmer, T.; Ward, T. R. *Angew. Chem., Int. Ed.* **2011**, *50*, 10863−10866.
(27) Zheng, L.; Baumann, U.; Reymond, J.-L. *Nucleic Acids Res.* **2004**, *32*, e115/1−e115/5.
(28) Humbert, N.; Zocchi, A.; Ward, T. R. *Electrophoresis* **2005**, *26*, 47−52.
(29) Åberg, J. B.; Samec, J. S. M.; Bäckvall, J.-E. *Chem. Commun. (Cambridge, U. K.)* **2006**, 2771−2773.
(30) Martins, J. E. D.; Clarkson, G. J.; Wills, M. *Org. Lett.* **2009**, *11*, 847−850.
(31) Václavík, J.; Kuzma, M.; Přech, J.; Kačer, P. *Organometallics* **2011**, *30*, 4822−4829.
(32) Blackmond, D. G.; Ropic, M.; Stefinovic, M. *Org. Process Res. Dev.* **2006**, *10*, 457−463.
(33) Marini-Bettolo, G. B.; Schmutz, J. *Helv. Chim. Acta* **1959**, *42*, 2146−2155.
(34) Ogata, Y.; Sawaki, Y. *J. Am. Chem. Soc.* **1973**, *95*, 4692−4698.
(35) Hocquaux, M.; Viel, C.; Brunaud, M.; Navarro, J.; Lacour, C.; Cazaubon, C. *Eur. J. Med. Chem.* **1983**, *18*, 331−338.
(36) Creus, M.; Pordea, A.; Rossel, T.; Sardo, A.; Letondor, C.; Ivanova, A.; LeTrong, I.; Stenkamp, R. E.; Ward, T. R. *Angew. Chem., Int. Ed.* **2008**, *47*, 1400−1404.